ANTIMICROBIAL AGENTS AND CHEMOTHERAPY, Nov. 2010, p. 4534–4539 Vol. 54, No. 11
0066-4804/10/$12.00 doi:10.1128/AAC.00643-10

Pharmacokinetics-Pharmacodynamics of a Respiratory Syncytial Virus Fusion Inhibitor in the Cotton Rat Model[▽]

Marie-Claude Rouan,[1] Tom Gevers,[1]* Dirk Roymans,[1] Loeckie de Zwart,[2] David Nauwelaers,[3] Marc De Meulder,[2] Pieter van Remoortere,[1] Marc Vanstockem,[1] Anil Koul,[2] Kenny Simmen,[1] and Koen Andries[2]

Tibotec BVBA, Johnson & Johnson, Generaal De Wittelaan L11B3, 2800 Mechelen, Belgium[1]; Johnson & Johnson Pharmaceutical Research and Development, Turnhoutseweg 30, 2340 Beerse, Belgium[2]; and Virco BVBA, Johnson & Johnson, Generaal De Wittelaan L11B3, 2800 Mechelen, Belgium[3]

Received 11 May 2010/Returned for modification 7 August 2010/Accepted 28 August 2010

Human respiratory syncytial virus (RSV) is a major cause of lower respiratory tract infections in infants, young children, elderly persons, and severely immunocompromised patients. Effective postinfection treatments are not widely available, and currently there is no approved vaccine. TMC353121 is a potent RSV fusion inhibitor *in vitro*, and its ability to reduce viral loads *in vivo* was demonstrated in cotton rats following prophylactic intravenous administration. Here, the pharmacokinetics of TMC353121 in the cotton rat, which is semipermissive for RSV replication, were further explored to build a pharmacokinetic-pharmacodynamic (PK-PD) model and to estimate the plasma drug levels needed for significant antiviral efficacy. TMC353121 reduced the viral titers in bronchoalveolar lavage fluid in a dose-dependent manner after a single subcutaneous administration and intranasal RSV inoculation 24 h after compound administration. The viral titer reduction and plasma TMC353121 concentration at the time of RSV inoculation were well described using a simple E_{max} model with a maximal viral titer reduction (E_{max}) of 1.5 $\log_{10}$. The plasma drug level required to achieve 50% of the E_{max} (200 ng/ml) was much higher than the 50% inhibitory concentration observed *in vitro* in HeLaM cells (0.07 ng/ml). In conclusion, this simple PK-PD approach may be useful in predicting efficacious exposure levels for future RSV inhibitors.

Since its first isolation from two hospitalized infants with severe lower respiratory tract infection, human respiratory syncytial virus (RSV) has emerged as an important human respiratory pathogen (5, 6, 12, 24). In many cases, infection is restricted to the upper respiratory tract and not associated with long-term pathology, but progression to a more severe lower respiratory tract infection in infants and children <6 years of age is frequent. Today, RSV is considered to be the main causative agent of lower respiratory tract infections such as bronchiolitis and pneumonia in infants and young children (12, 16, 23, 24). In healthy adults, infection usually causes symptoms similar to those of the common cold, but in hospitalized elderly or severely immunocompromised patients, RSV is a significant pathogen, often resulting in pneumonia and high mortality rates (11, 25).

In spite of extensive efforts, development of an anti-RSV vaccine has proven to be particularly challenging and has not been successful to date (22, 26). Prophylactic options are limited to passive immunization with the humanized monoclonal antibody Synagis. However, administration of Synagis is restricted to at-risk infants <2 years old. For therapeutic intervention, the antiviral drug ribavirin is the only option, but its use is limited due to its problematic mode of administration as an aerosol, its limited efficacy, and its teratogenicity (15). Hence, effective therapeutic options are needed for treatment of the at-risk population, including adults and the elderly.

Several animal models have been established to study RSV pathogenesis and treatment (4). However, no single animal model presents the complete spectrum of the disease observed in humans. Several primate models have been successfully used to demonstrate the prophylactic or therapeutic efficacy of human RSV antivirals (8, 9, 14, 17). Small-rodent models of human RSV infection such as BALB/c mice and cotton rats (*Sigmodon hispidus*) have not only contributed to the understanding of the pathogenesis and immunobiology of human RSV disease but have also been used to demonstrate the *in vivo* efficacy of antiviral agents (1, 7, 10, 13, 14, 19, 20, 27, 28). Replication of human RSV in cotton rats is restricted, and a large inoculum of virus is required to achieve a modest degree of virus replication (9). This semipermissiveness of the cotton rat model is probably its biggest disadvantage, resulting in viral replication kinetics that are quite different from those of the primate or human situation. Only a few pharmacokinetic-pharmacodynamic (PK-PD) results in rodent and primate RSV models have been reported, and thus it is still unclear how the relationship between viral titer reduction and systemic exposure translates from these *in vivo* models to patients infected with RSV.

Previously, we reported the discovery of TMC353121, a potent human RSV inhibitor, and demonstrated its activity *in vivo* (3). The pharmacokinetics of TMC353121 in cotton rats were further explored in order to build a PK-PD model, and the results obtained are described in this paper.

* Corresponding author. Mailing address: Tibotec BVBA, Turnhoutseweg 30, 2340 Beerse, Belgium. Phone: 32(0)14 60 51 07. Fax: 32(0)14 60 54 03. E-mail: tgevers@its.jnj.com.

▽ Published ahead of print on 7 September 2010.

MATERIALS AND METHODS

Viruses. The Long strain of RSV was obtained from ATCC (Manassas, VA). The virus was propagated in HeLaM cells, and infectious RSV titers were determined by plaque assay as previously described (1) and by quantitative reverse transcriptase PCR (qRT-PCR) assay as described below.

Animals. Cotton rats and Sprague-Dawley rats were purchased from Charles River Laboratories (Brussels, Belgium). Cotton rats of either sex weighing 60 to 100 g and 5 to 15 weeks of age and male Sprague-Dawley rats weighing 200 to 300 g and 7 to 10 weeks of age were used. All animals were housed individually under controlled conditions (specific pathogen free, 23°C, 60% humidity, normal light-dark cycle) and had access to food and water *ad libitum*. All efforts were made to minimize animal discomfort and limit the number of animals used. The local Johnson & Johnson Ethical Committee approved all experimental protocols, and the actual experiments were carried out following the procedure described by the guidelines of the European Community Council directive of 24 November 1986 (Declaration of Helsinki 86/609/EEC).

Pharmacokinetic experiments. Sprague-Dawley and cotton rats were given a single-bolus dose of 10 mg/kg TMC353121 intravenously (i.v.). TMC353121 was dissolved in an aqueous 10% 2-hydroxypropyl-β-cyclodextrin solution at pH 4. Blood samples were taken from the orbital venous plexus of three Sprague-Dawley rats at 15 min and 1, 8, and 24 h postdose and from six Sprague-Dawley rats and six cotton rats at 3 h postdose. Blood samples were centrifuged at 1,500 × *g* for 10 min, and plasma was separated and frozen until bioanalysis. After blood sampling, the rats were exsanguinated from the vena femoralis under isoflurane-oxygen anesthesia. Then they were euthanized by CO_2 asphyxiation, and the lungs were subjected to lavage once via a tracheal cannula with phosphate-buffered saline (PBS) containing 2% bovine serum albumin (BSA) at room temperature at a volume of 5 ml per Sprague-Dawley rat or 2.5 ml per cotton rat. After gentle injection of the lavage fluid into the lungs, the fluid was withdrawn for collection of the bronchoalveolar lavage fluid (BALF) and the lungs were dissected. BALF was collected in order to assess TMC353121 concentrations in the lung epithelial lining fluid (ELF) after correction for the dilution with lavage fluid. A single lavage with a short dwelling time was applied as previously recommended for better accuracy of the determination of ELF dilution (2). BSA was added to the lavage fluid in order to prevent the adsorption of TMC353121 to syringes or other containers. The BALF was centrifuged at 300 × *g* for 10 min, and the supernatant was separated. BALF supernatant and lung tissue samples were then frozen until bioanalysis. BALF supernatant is referred as BALF throughout this paper.

In a separate study, six Sprague-Dawley rats were given a single dose of 50 mg/kg subcutaneously (s.c.). An aqueous, slow-release nanocrystal suspension of TMC353121 was administered. Polysorbate 80 and sodium deoxycholate were used as stabilizers. TMC353121 was sterilized by gamma irradiation and surfactant solutions were sterile filtered. The formulation process was made under "best-clean" conditions. When characterized with a Malvern Mastersizer 2000 (Malvern Instruments Ltd., Worcestershire, United Kingdom) and expressed as a volume distribution, 99% of the nanocrystals were <300 nm. Blood samples were taken from the orbital venous plexus at 1, 3, 7, 24, 48, and 72 h after dosing. Blood samples were centrifuged at 1,500 × *g* for 10 min. Plasma was separated and frozen until bioanalysis.

PK-PD experiment. Five cohorts of six cotton rats were given the aqueous nanocrystal suspension of TMC353121 in a single s.c. dose of 12.5, 25, 50, 100, or 200 mg/kg. An additional group of six nontreated control rats was included. Blood samples were obtained from the orbital venous plexus 24 h after the administration of TMC353121 and centrifuged at 1,500 × *g* for 10 min. Plasma was separated and frozen until bioanalysis. Immediately after blood collection, rats were anesthetized with isoflurane and inoculated dropwise by the intranasal route with 10^6 PFU of RSV in 0.1 ml cell culture medium. Four days after RSV inoculation, all test animals were euthanized by CO_2 gas asphyxiation. The lungs of the animals were intubated and flushed once with 2.5 ml PBS, and the BALF was centrifuged at 300 × *g* for 10 min. The resulting supernatant was titrated immediately for RSV infectivity by plaque and qRT-PCR assays as described below.

Plaque assay for determination of RSV titers in BALF. The BALF supernatant was titrated on Vero cells. Briefly, $\log_{10}$ dilutions of the supernatants were added to Vero cell monolayers in six-well Falcon plates (BD, Erembodegem, Belgium) and incubated at 37°C for 1 h. After one wash step with PBS, the inoculum was replaced with 3 ml agarose growth medium and the incubation was continued at 37°C. After 7 days, the cells were fixed with Formol and stained with a 0.4% methylene blue solution. Plaques were counted, and the titer was expressed as $\log_{10}$ PFU/ml BALF and then corrected for dilution with lavage fluid and converted to $\log_{10}$ PFU/ml ELF as mentioned below. The antiviral effect was calculated as $\log_{10}$ titer reduction compared to the titer of untreated control rats.

qRT-PCR assay for determination of RSV titers in BALF. One volume of 10% dithiothreitol (Acros Organics, Geel, Belgium) in PBS (Invitrogen, Merelbeke, Belgium) and 4 volumes of NucliSens extraction lysis buffer (bioMérieux, Boxtel, Netherlands) were added to the BALF samples, and then they were incubated for 10 min. A combination of 3 ml lysed sample and 100 μl of extraction control mix containing 50 μl NucliSens magnetic beads (bioMérieux), 10 μl internal extraction control (IEC) RNA (see below), and 40 μl NucliSens Extraction Buffer 3 (bioMérieux) was extracted on an EasyMAG apparatus (bioMérieux). Elution was done in 110 μl.

Monoplex real-time qRT-PCR mixtures (final volume, 35 μl) contained 10 μl extracted RNA, 0.360 μl yeast tRNA (Invitrogen), 150 μl 2× EuroScript reaction buffer (Eurogentec, Liege, Belgium), 0.15 μl Euroscript RT (Eurogentec), 0.1 μM probe (6-carboxyfluorescein [FAM]-5′-CAGACTACTAGAGATTACC-3′-nonfluorescent quencher [NFQ]-minor groove binding molecule [MGB]), 0.9 μM each primer (forward, 5′-CTGTGATAGARTTCCAACAAAAGAACA-3′; reverse, 5′-AGTTACACCTGCATTAACACTAAATTCC-3′), 1.5 mM $MgCl_2$, and RNase/DNase-free water (Invitrogen). Amplification and detection were performed in an ABI 7900HT (Applied Biosystems, Foster City, CA). All quantifications were performed in duplicate. A total of eight 10-fold serial dilutions of an RSV RNA standard were processed in duplicate on each real-time PCR plate with the same reaction mixture used to process the samples, in order to determine the dynamic range and performance of the real-time PCR reagents during each run. RNA extraction efficiency was determined by amplification of the IEC RNA in parallel reaction mixtures in the same sample plates and with the same sample master mix using the following primers and probe: 5′-GGCTCCAGAA TATAGGCATGATTC-3′ (forward primer), 5′-TGGTTATTACAAGAGCAG CTATACACAGT-3′ (reverse primer), and FAM-5′-TACCGTACTCTAGCCT A-3′-NFQ-MGB (probe). The IEC $C_{T\text{Batch Value}}$ (where C_T is the threshold cycle) was determined by repeated measurements of >700 IEC RNA aliquots. To correct for loss of RNA during the extraction process, the following formula was used: $C_{T\text{Sample}}$ − (IEC $C_{T\text{Sample}}$ − IEC $C_{T\text{Batch Value}}$).

Determination of TMC353121 in plasma, BALF, and lung tissue. Plasma, BALF, and lung tissue homogenate samples from cotton rat studies were spiked with a stable-isotope-labeled internal standard and precipitated with acetonitrile. An aliquot of the supernatant was injected onto a liquid chromatograph coupled to a tandem mass spectrometer for analysis. The column used was a Varian Polaris C18-A (50 by 4.6 mm; Palo Alto, CA) packed with 3-μm-diameter particles operating at ambient temperature with a flow rate of 1 ml/min. The mobile phase consisted of 0.1 M ammonium formate adjusted to pH 4 with formic acid and acetonitrile. A 10-point standard curve in the same matrix as the study samples was constructed from 0.2 to 200 ng/ml plasma or BALF and from 100 to 100,000 ng/g lung tissue, respectively.

Conversion from BALF to ELF concentrations and titers. Bronchoalveolar lavage was used for sampling of the ELF of the lower respiratory tract. BALF consisted of ELF diluted in the fluid that was used to perform the lavage. Compound concentrations and RSV titers in ELF were determined from the concentrations in BALF and the dilution with lavage fluid. The dilution was calculated using urea as an endogenous marker. Urea concentrations in serum and BALF were measured with the Urea Berthelot colorimetric assay kit (Ecoline 131159990305; DiaSys, Holzheim, Germany). Compound concentrations and RSV titers in ELF were calculated as follows: compound concentration or RSV titer in BALF × (serum urea concentration/BALF urea concentration).

Data analysis. The following pharmacokinetic parameters were calculated from the mean plasma drug concentrations determined after i.v. bolus administration using noncompartmental analysis (WinNonlin; Pharsight, Mountain View, CA): the area under the plasma drug concentration-time curve from time zero to 24 h postdose ($AUC_{0\text{-}24\ h}$) using the linear up/log down trapezoidal rule, the systemic clearance (CL) calculated as dose/AUC, the apparent volume of distribution at steady state (V_{ss}) calculated as CL × AUMC/AUC. AUC is the area under the curve extrapolated to infinity using the half-life determined between 8 and 24 h, and AUMC is the corresponding area under the first-moment curve. The values of $AUC_{0\text{-}24\ h}$ were also determined from the mean drug concentrations in BALF and lung tissue. After s.c. drug administration to cotton rats, the simple E_{max} model was used to describe the relationship between viral titer reduction and the plasma TMC353121 concentration at 24 h postdose ($C_{24\ h}$) corresponding to the time of virus inoculation, by applying the equation $E = (E_{max} \times C_{24\ h})/(C_{24\ h} + EC_{50})$. E is the observed antiviral effect (viral titer reduction expressed as $\log_{10}$ PFU/ml ELF), E_{max} is the maximum pharmacological effect, and EC_{50} is the plasma TMC353121 concentration required to produce 50% of the E_{max}. WinNonlin was used to fit the pool of the individual data.

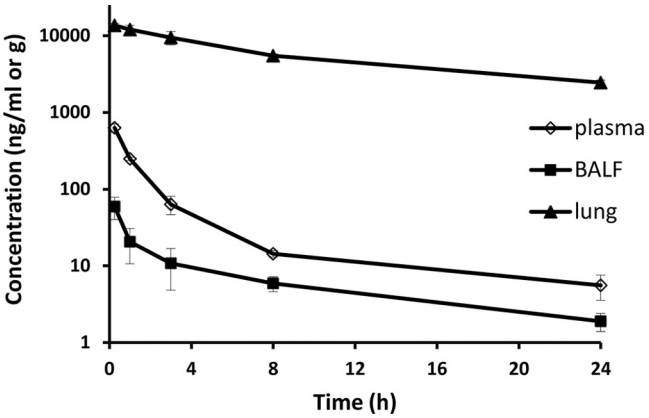

FIG. 1. Mean ± SD TMC353121 concentrations in the plasma, BALF, and lung tissue of Sprague-Dawley rats following a single i.v. bolus administration (10 mg/kg). Each symbol represents the mean concentration from three rats, except at 3 h postdose ($n = 6$).

RESULTS

Pharmacokinetics after i.v. dosing. After i.v. bolus administration of a single dose of 10 mg/kg to Sprague-Dawley rats, the plasma drug concentration-time profile of TMC353121 exhibited multicompartmental pharmacokinetics. Mean plasma drug concentrations decreased rapidly during the first hours after dosing and then more slowly, with a half-life of about 12 h, as determined for the last part of the curve between 8 and 24 h postdose (Fig. 1). TMC353121 was rapidly eliminated from plasma (CL = 8.6 liters/h/kg) and extensively distributed (V_{ss} = 55 liters/kg) (Table 1). ELF dilution could not be determined in Sprague-Dawley rats because the urea concentrations in the BALF were below the limit of quantification. Therefore, the TMC353121 concentrations in BALF were plotted versus time as an indication of the time course of the concentrations in ELF (Fig. 1). TMC353121 concentrations in BALF and lung tissue reached their maxima as early as the first sampling time point (15 min), indicating fast distribution. Lung tissue drug concentrations were much higher than plasma drug concentrations (lung-to-plasma $AUC_{0\text{-}24\ h}$ ratio, 122), whereas drug concentrations in BALF were lower than drug concentrations in plasma at all time points. Drug concentrations in both lung tissue and BALF decreased more slowly than those in plasma within the first 8 h postdose (the plasma/BALF ratio was 10 at 15 min and at 1 h postdose and 2.5 at 8 h postdose). Between 8 and 24 h postdose, the concentration-time profiles in plasma, lung tissue, and BALF were parallel, ELF concentration-time profiles being expected to follow the same kinetics. The high lung tissue drug concentrations are in agreement with the high volume of distribution mentioned above. Even higher concentrations were found in lungs and livers in repeated-dose rat and dog studies without any histological evidence of compound precipitation. TMC353121 is a lipophilic compound. Because of its weak basic properties, it is trapped in its protonated form in acidic cell compartments (e.g., lysosomes), resulting in high concentrations in lysosome-rich tissues such as those of the lung and liver, from which it is slowly released.

TABLE 1. Pharmacokinetic parameters of TMC353121 in Sprague-Dawley rats following a single-bolus i.v. administration of 10 mg/kg

Matrix	$AUC_{0\text{-}24\ h}$ (ng/h/ml)	CL (liters/h/kg)	V_{ss} (liters/kg)
Plasma	1,100	8.6	55
Lung tissue	131,000		
BALF	170		

TABLE 2. TMC353121 concentrations in plasma, lung tissue, BALF, and ELF of Sprague-Dawley rats and cotton rats at 3 h after a single-bolus i.v. administration of 10 mg/kg

Rat type	TMC353121 concn (ng/ml)[a] in:			
	Plasma	Lung tissue	BALF	ELF
Sprague-Dawley	63 ± 17	9,400 ± 1,800	11 ± 6	
Cotton	111 ± 130	4,700 ± 1,600	23 ± 10	392 ± 147

[a] Values are mean ± standard deviation ($n = 6$ animals).

In cotton rats given a single-bolus i.v. dose of 10 mg/kg, the variability of TMC353121 concentrations determined in plasma at 3 h postdose was higher than in Sprague-Dawley rats (Table 2). Only up-to-2-fold differences in mean plasma, lung tissue, and BALF drug concentrations between the two strains were observed. Unlike in Sprague-Dawley rats, urea concentrations in the BALF of cotton rats were quantifiable. The mean dilution ± standard deviation (SD) with the lavage fluid was 18 ± 5, rendering a mean lung ELF drug concentration of 392 ± 147 ng/ml, i.e., 3.5-fold higher than the corresponding mean plasma drug concentration.

Pharmacokinetics after s.c. dosing. After single s.c. administration of a sustained-release nanocrystal formulation (50 mg/kg) to Sprague-Dawley rats, mean plasma TMC353121 concentrations reached a maximum at around 3 h postdose and remained on a plateau at 40 to 55 ng/ml between 3 and 24 h. Thereafter, drug concentrations decreased slowly to reach 48-h values only about 2-fold lower than the 24-h values (Fig. 2).

Following a single s.c. administration of 12.5, 25, 50, 100, or 200 mg/kg to cotton rats, the plasma TMC353121 concentrations determined at 24 h appeared to increase approximately linearly with the dose, although the interanimal variability was rather high (Fig. 3).

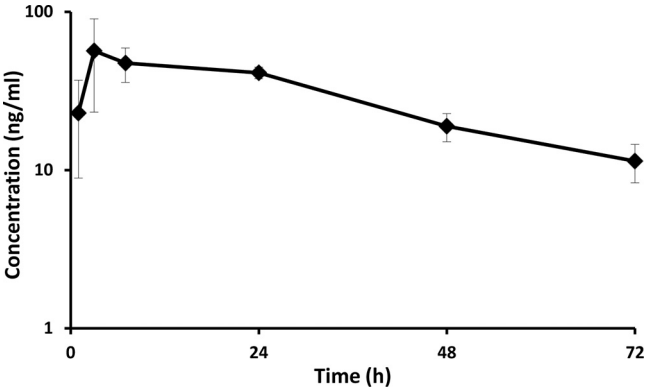

FIG. 2. Mean ± SD plasma TMC353121 concentrations ($n = 6$) in Sprague-Dawley rats following a single s.c. administration of a sustained-release formulation (50 mg/kg).

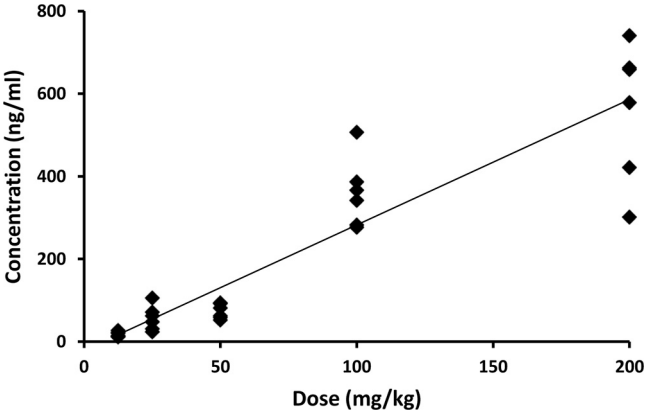

FIG. 3. Plot of individual plasma TMC353121 concentrations determined in cotton rats 24 h after a single s.c. administration of a sustained-release formulation versus the dose. The doses given to cohorts of six animals were 12.5, 25, 50, 100, and 200 mg/kg. The solid line shows the fit of the data points by linear regression analysis (coefficient of correlation, 0.92).

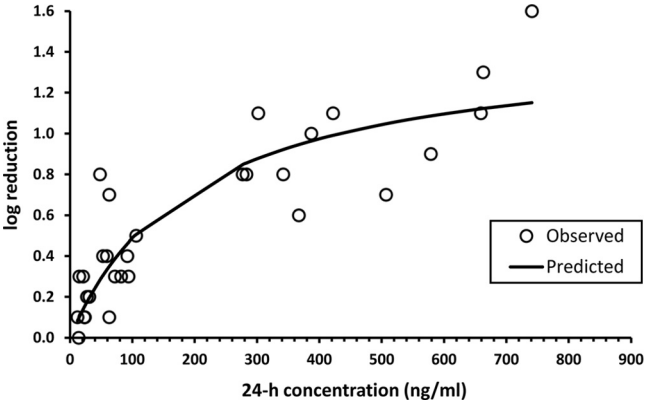

FIG. 5. Relationship between the viral titer reduction (expressed as $\log_{10}$ PFU/ml ELF reduction) versus the plasma TMC353121 concentration in cotton rats at the time of challenge (24 h after s.c. administration of a single dose of 12.5, 25, 50, 100, or 200 mg/kg). The open circles represent the individual experimental values, and the solid line represents the model-derived relationship as determined using a simple E_{max} model.

Antiviral activity in cotton rats after s.c. dosing. The antiviral activity of TMC353121 was examined in a dose-ranging study with cotton rats. Cohorts of six animals were administered the nanocrystal formulation in s.c. doses of 12.5, 25, 50, 100, and 200 mg/kg 24 h before virus inoculation. Four days later, BALF samples were collected and RSV titers were determined by plaque and qRT-PCR assays. The viral load in untreated control animals was 5.6 $\log_{10}$ PFU/ml ELF. Compared to the titers of untreated control rats, significant (P values < 0.05) reductions of 0.2, 0.3, 0.4, 0.8, and 1.2 $\log_{10}$ PFU/ml ELF were measured by plaque assay and of 0.5, 0.6, 1.1, 1.7, and 2.2 $\log_{10}$ PFU/ml ELF were measured by qRT-PCR assay after administration of the above-mentioned doses, respectively (Fig. 4). Across samples treated with different concentrations of TMC353121, the treatment effect was less pronounced when assessed by quantitative plaque titration, than when assessed by qRT-PCR. The observed difference is unlikely to be due to nonspecific inhibition of the viral replication in the plaque assay since TMC353121-treated and control samples were processed identically. The difference may be related to the fact that the plaque assay monitors infectious viral particles only, while the qRT-PCR assay estimates viral RNA from both infectious and noninfectious virions, as well as viral transcripts released from infected host cells (18).

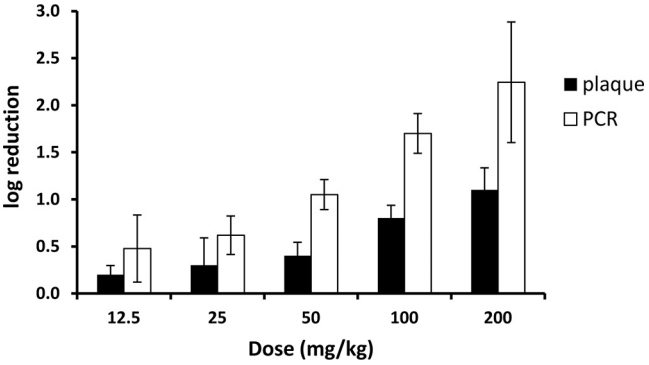

FIG. 4. Efficacy of s.c. TMC353121 against RSV in the cotton rat model. Animals were inoculated intranasally with the RSV Long strain. The compound was administered s.c. 24 h before RSV inoculation at doses varying from 12.5 to 200 mg/kg. The control group was inoculated with RSV but not treated with TMC353121. RSV titers determined by plaque and qRT-PCR assays and are expressed as $\log_{10}$ PFU/ml ELF. The mean ± SD log reduction in the titer of each dose group versus that of the untreated control group is presented.

PK-PD relationship after s.c. dosing. The individual viral titer reduction values determined by plaque assay after s.c. administration of single doses of 12.5, 25, 50, 100, and 200 mg/kg to cotton rats were plotted versus the corresponding plasma TMC353121 concentration determined at 24 h postdose, prior to virus inoculation (Fig. 5). The relationship between viral titer reduction (E) and the 24-h plasma drug concentration ($C_{24\ h}$) was well described by the simple E_{max} model by applying the equation $E = (E_{max} \times C_{24\ h})/(C_{24\ h} + EC_{50})$. E_{max} derived from the model corresponded to a $\log_{10}$ viral titer reduction of 1.5 (Table 3), and the EC_{50} was 200 ng/ml.

DISCUSSION

Anti-RSV activity of TMC353121 has previously been demonstrated in cotton rats following i.v. bolus administration (3). A significant viral load reduction was obtained after a single administration of TMC353121. The maximum antiviral effect was achieved when the compound was administered shortly (i.e., 5 min) before the virus challenge, consistent with its

TABLE 3. Estimates of the parameters of the E_{max} model

Parameter	E_{max} ($\log_{10}$ reduction)[a]	EC_{50} (ng/ml)
Estimate	1.5	200
SD	0.20	71
CV[b] (%)	14	35

[a] The E_{max} model equation $(E_{max} \times C_{24h})/(C_{24h} + EC_{50})$ was used to fit the individual viral titer reduction values versus the plasma TMC353121 concentration at the time of challenge (24 h after s.c. administration).

[b] CV, coefficient of variation.

mechanism of action and its activity in single-round time-of-addition experiments (21). Moreover, the amount of virus recovered from the lungs in the cotton rat host model has been shown to be directly proportional to the amount of challenge virus (20). This suggests that the cotton rat is semipermissive for RSV infection, involving limited replication with very likely just one round of replication. TMC353121 has to be present before completion of the virus-host cell fusion process. Therefore, a PK-PD relationship can be established in the cotton rat following a single drug administration and using the concentration of TMC353121 in the effect compartment at the time of challenge. As TMC353121 blocks viral entry, it has an extracellular activity and ELF appears to be the most relevant effect compartment. This is supported by the small viral load reduction obtained in cotton rats when an RSV challenge was given 24 h after a single i.v. TMC353121 administration (3), in agreement with the low ELF concentrations at the time of challenge, but not with the high lung tissue drug concentrations (>2,000 ng/ml in Sprague Dawley rats, as shown in Fig. 1).

Kinetics of TMC353121 elimination and distribution to lung tissue and ELF were characterized after i.v. bolus administration. Sprague-Dawley rats were used to characterize the concentration-time profiles because these animals are easier to handle than cotton rats. The plasma drug profiles obtained after i.v. bolus administration were previously shown to be roughly comparable in the two rat types (unpublished data). Following i.v. administration of a single dose of 10 mg/kg to Sprague-Dawley rats, TMC353121 was eliminated rapidly from plasma with a systemic clearance higher than the hepatic blood flow and was extensively distributed. Despite extensive metabolism, unchanged TMC353121 was by far the major circulating compound (unpublished data). The slower decline of lung and ELF TMC353121 concentrations within the first 8 h postdose, compared to plasma drug concentrations, suggests that lung tissue and ELF constitute deep compartments. The parallel time courses of the drug concentrations in plasma, lung tissue, and ELF between 8 and 24 h reflect a slow release of TMC353121 from deep compartments and indicate that the distribution equilibrium was achieved at 8 h, with the lung/plasma or ELF/plasma drug concentration ratio remaining constant. Therefore, the plasma drug concentration at 8 h or later time points after a single administration can be used as a surrogate for the ELF drug concentration for PK-PD application, i.e., when a plasma/ELF distribution equilibrium is achieved.

I.v. administration of TMC353121 is not suitable to study PK-PD relationships because plasma drug concentrations decrease rapidly within the first hours after injection, rendering low plasma drug concentrations at 8 h postdose when a distribution equilibrium is achieved, as shown in Fig. 1. Only a slight viral load reduction was obtained when the challenge was given at 8 h postdose or later time points (unpublished data). Therefore, TMC353121 was administered s.c. as a sustained-release formulation, resulting in a much slower plasma drug concentration decline, and in concentrations sufficiently high to obtain a significant viral load reduction. Inoculation of the virus was performed at 24 h after drug administration, when distribution equilibrium was achieved. The RSV load reduction determined by plaque assay and the plasma drug concentration at the time of challenge were well described by using a simple E_{max} model with a model-derived value of a 1.5-$\log_{10}$ reduction for E_{max}. Plasma drug concentrations of >1,000 ng/ml could not be reached by s.c. administration because 200 mg/kg was the maximum feasible dose. However, a maximum TMC353121 antiviral effect (1.5- to 1.6-$\log_{10}$ reduction) similar to E_{max} has been obtained previously in cotton rats following a single i.v. or inhalation administration (3), thereby confirming the model-derived value of E_{max}.

In vitro, TMC353121 is active against wild-type RSV (strain LO), with a 50% effective concentration (*in vitro* EC_{50}) of 0.07 ng/ml in HeLaM cells (3). In the cotton rat, 50% of the maximum antiviral activity was achieved at a plasma drug concentration of 200 ng/ml, which is significantly higher than the *in vitro* EC_{50}, even when adjusted for 99% plasma protein binding (7 ng/ml). Significant efficacy was also obtained in cotton rats at high plasma drug concentrations for another RSV fusion inhibitor, BMS-433771 (*in vitro* EC_{50} of 20 nM) (5). After a single oral administration of BMS-433771 1 h prior to RSV inoculation, a significant viral load reduction of 1.0 $\log_{10}$ was obtained for an AUC value of 5,000 ng/h/ml.

In conclusion, TMC353121 was shown to reduce the RSV load in a dose-dependent manner following a single s.c. administration in the cotton rat model. A simple PK-PD model was used to estimate the plasma TMC353121 level necessary to obtain a significant RSV titer reduction, with the advantage of a single administration and a single PK sampling at the time of RSV inoculation. This model can be a useful tool for the evaluation of RSV fusion inhibitors. The relationship between the plasma drug levels required to achieve significant antiviral activity in the cotton rat and in different clinical situations still needs to be evaluated.

REFERENCES

1. **Andries, K., M. Moeremans, T. Gevers, R. Willebrords, C. Sommen, J. Lacrampe, F. Janssens, and P. R. Wyde.** 2003. Substituted benzimidazoles with nanomolar activity against respiratory syncytial virus. Antiviral Res. **60:**209–219.
2. **Bayat, S., K. Louchahi, B. Verdière, D. Anglade, A. Rahoui, P. M. Sorin, M. Tod, O. Petitjean, F. Fraisse, and F. A. Grimbert.** 2004. Comparison of ^{99m}Tc-DTPA and urea for measuring cefepime concentrations in epithelial lining fluid. Eur. Respir. J. **24:**150–156.
3. **Bonfanti, J. F., C. Meyer, F. Doublet, J. Fortin, P. Muller, L. Queguiner, T. Gevers, P. Janssens, H. Szel, R. Willebrords, P. Timmerman, K. Wuyts, P. van Remoortere, F. Janssens, P. Wigerinck, and K. Andries.** 2008. Selection of a respiratory syncytial virus fusion inhibitor clinical candidate. 2. Discovery of a morpholinopropylaminobenzimidazole derivative (TMC353121). J. Med. Chem. **51:**875–896.
4. **Byrd, L. G., G. A. Prince.** 1997. Animal models of respiratory syncytial virus infection. Clin. Infect. Dis. **25:**1363–1368.
5. **Chanock, R., and L. Finberg.** 1957. Recovery from infants with respiratory illness of a virus related to chimpanzee coryza agent (CCA). II. Epidemiologic aspects of infection in infants and young children. Am. J. Hyg. (Lond.) **66:**291–300.
6. **Chanock, R., B. Roizman, and R. Myers.** 1957. Recovery from infants with respiratory illness of a virus related to chimpanzee coryza agent (CCA). I. Isolation, properties and characterization. Am. J. Hyg. (Lond.) **66:**281–290.
7. **Cianci, C., E. V. Genovesi, L. Lamb, I. Medina, Z. Yang, L. Zadjura, H. Yang, C. D'Arienzo, N. Sin, K.-L. Yu, K. Combrink, Z. Li, R. Colonno, N. Meanwell, J. Clark, and M. Krystal.** 2004. Oral efficacy of a respiratory syncytial virus inhibitor in rodent models of infection. Antimicrob. Agents Chemother. **48:**2448–2454.
8. **Cramer, H., J. R. Okicki, M. Kuang, and Z. Xu.** 2005. Targeted therapy of respiratory syncytial virus by 2-5A antisense. Nucleosides Nucleotides Nucleic Acids **24:**497–501.
9. **Davis, C. B., T. W. Hepburn, J. J. Urbanski, D. C. Kwok, T. K. Hart, D. J. Herzyk, S. G. Demuth, M. Leland, and G. R. Rhodes.** 1995. Preclinical pharmacokinetic evaluation of the respiratory syncytial virus-specific reshaped human monoclonal antibody RSHZ19. Drug Metab. Dispos. **23:** 1028–1036.
10. **Domachowske, J. B., C. A. Bonville, and H. F. Rosenberg.** 2004. Animal

models for studying respiratory syncytial virus infection and its long term effects on lung function. Pediatr. Infect. Dis. J. **23:**S228–234.
11. **Falsey, A. R., and E. E. Walsh.** 2000. Respiratory syncytial virus infection in adults. Clin. Microbiol. Rev. **13:**371–384.
12. **Hall, C. B., K. R. Powell, N. E. MacDonald, C. L. Gala, M. E. Menegus, S. C. Suffin, and H. J. Cohen.** 1986. Respiratory syncytial virus infection in children with immunocompromised immune function. N. Engl. J. Med. **315:**77–81.
13. **Hruska, J. F., P. E. Morrow, S. C. Suffin, and R. G. Douglas.** 1982. In vivo inhibition of respiratory syncytial virus by ribavirin. Antimicrob. Agents Chemother. **21:**125–130.
14. **Huntley, C. C., W. J. Weiss, A. Gazumyan, A. Buklan, B. Feld, W. Hu, T. R. Jones, T. Murphy, A. A. Nikitenko, B. O'Hara, G. Prince, S. Quartuccio, Y. E. Raifeld, P. Wyde, and J. F. O'Connell.** 2002. RFI-641, a potent respiratory syncytial virus inhibitor. Antimicrob. Agents Chemother. **46:**841–847.
15. **Kochhar, D. M., J. D. Penner, and T. B. Knudsen.** 1980. Embryotoxic, teratogenic, and metabolic effects of ribavirin in mice. Toxicol. Appl. Pharmacol. **52:**99–112.
16. **Leader, S., and K. Kohlhase.** 2002. Respiratory syncytial virus-coded pediatric hospitalizations, 1997 to 1999. Pediatr. Infect. Dis. J. **21:**629–632.
17. **Leaman, D. W., F. J. Longano, J. R. Okicki, K. F. Soike, P. F. Torrence, R. H. Silverman, and H. Cramer.** 2002. Targeted therapy of respiratory syncytial virus in African green monkeys by intranasally administered 2-5A antisense. Virology **292:**70–77.
18. **Perkins, S. M., D. L. Webb, S. A. Torrance, C. El Saleeby, L. M. Harrison, J. A. Aitken, A. Patel, and J. P. DeVincenzo.** 2005. Comparison of a real-time reverse transcriptase PCR assay and a culture technique for quantitative assessment of viral load in children naturally infected with respiratory syncytial virus. J. Clin. Microbiol. **43:**2356–2362.
19. **Prince, G. A., V. G. Hemming, R. L. Horswood, and R. M. Chanock.** 1985. Immunoprophylaxis and immunotherapy of respiratory syncytial virus infection in the cotton rat. Virus Res. **3:**193–206.
20. **Prince, G. A., A. B. Jenson, R. L. Horswood, E. Camargo, and R. M. Chanock.** 1978. The pathogenesis of respiratory syncytial virus infection in cotton rats. Am. J. Pathol. **93:**771–791.
21. **Roymans, D., H. L. De Bondt, E. Arnoult, P. Geluykens, T. Gevers, M. Van Ginderen, N. Verheyen, H. Kim, R. Willebrords, J. F. Bonfanti, W. Bruinzeel, M. D. Cummings, H. van Vlijmen, and K. Andries.** 2010. Binding of a potent small-molecule inhibitor of six-helix bundle formation requires interactions with both heptad-repeats of the RSV fusion protein. Proc. Natl. Acad. Sci. U. S. A. **107:**308–313.
22. **Schmidt, A. C.** 2007. Progress in respiratory virus vaccine development. Semin. Respir. Crit. Care Med. **28:**243–252.
23. **Shay, D. K., R. C. Holman, R. D. Newman, L. L. Liu, J. W. Stout, and L. J. Anderson.** 1999. Bronchiolitis-associated hospitalizations among US children, 1980-1996. JAMA **282:**1440–1446.
24. **Simoes, E. A. F.** 1999. Respiratory syncytial virus infection. Lancet **354:**847–852.
25. **Thompson, W. W., D. K. Shay, E. Weintraub, L. Brammer, N. Cox, L. J. Anderson, and K. Fukuda.** 2003. Mortality associated with influenza and respiratory syncytial virus in the United States. JAMA **289:**179–186.
26. **van Drunen Littel-van den Hurk, S., J. W. Mapletoft, N. Arsic, and J. Kovacs-Nolan.** 2007. Immunopathology of hRSV infection: prospects for developing vaccines without this complication. Rev. Med. Virol. **17:**5–34.
27. **Wu, H., D. S. Pfarr, S. Johnson, Y. A. Brewah, R. M. Woods, N. K. Patel, W. I. White, J. F. Young, and P. A. Kiener.** 2007. Development of motavizumab, an ultra-potent antibody for the prevention of respiratory syncytial virus infection in the upper and lower respiratory tract. J. Mol. Biol. **368:**652–665.
28. **Wyde, P. R., S. Laquerre, S. N. Chetty, B. E. Gilbert, T. J. Nitz, and D. C. Pevear.** 2005. Antiviral efficacy of VP14637 against respiratory syncytial virus in vitro and in cotton rats following delivery by small droplet aerosol. Antiviral Res. **68:**18–26.